RECURSIVE ENHANCEMENT OF NONCAUSAL IMAGES *

Nikhil Balram *José M. F. Moura*

LASIP, Depart. Elect. and Comp. Eng., Carnegie Mellon University, Pittsburgh, PA, 15213.

Abstract

In this paper, we implement a recursive procedure for the enhancement of noncausal Gauss Markov random fields. Experimental results for the enhancement of synthetic as well as real images corrupted by additive white Gaussian noise are provided. These are contrasted with equivalent results obtained by processing the images with recursive filters derived by imposing a causality constraint upon the fields. The results show that the noncausal recursors provide considerable reduction in the mean square error (MSE) of the noisy images without the introduction of undesirable visual effects, such as streaking, that are produced when causality constraints are imposed.

1. Introduction

In almost any form of image acquisition some degree of noise degradation is unavoidable. Consequently, image enhancement procedures are required to improve the image quality. For practical purposes these procedures must be fast as well as optimal. This is the problem we address in this paper.

Since, in general, images are noncausal phenomena, we model them using noncausal Markov random fields. Such models have been widely used for image processing applications, see, for e.g., [1], [2]. For reasons of computational efficiency, recursive image processing algorithms are desirable, but those that have been implemented are based on causal 2D fields, see, for e.g., [3]. The use of causal field models to process noncausal images produces undesirable effects, such as streaking, in the processed images. As an alternative, in this paper we implement an optimal recursive enhancement procedure based on a noncausal image field model. This produces significant improvement in the mean square error (MSE) of the noisy images without introducing undesired artifacts.

*The work reported here was partially supported by NSF grant # CDA-8820575 and by ONR grant # N0014-91-J-1001

Our approach makes use of a recursive framework for noncausal finite lattice Gauss Markov Random Fields (GMRF) that was developed recently, see [4], [5]. The noncausal field parameters are estimated from the image data using Maximum Likelihood (ML) estimation. Then the recursive framework is applied to produce an equivalent one–sided model which provides the basis for the Rauch–Tung–Striebel (RTS) formulation of the optimal fixed interval smoother.

The approach is demonstrated using synthetic and real images corrupted by additive white Gaussian noise. The visual quality of the results produced using noncausal image field models is compared with that of the corresponding results produced using causal field models.

The organization of the paper is as follows. The recursive framework for noncausal finite lattice GMRFs is briefly reviewed in section 2, and a sample of a noncausal field synthesized using this framework is provided. In section 3, the procedure that is followed for recursive enhancement of noisy images is described, along with the results of experiments conducted using a synthesized image as well as a real image. Conclusions are presented in section 4.

2. Recursive framework

It has been shown that a noncausal finite lattice GMRF can be characterized by the structure of its inverse covariance matrix, A, which we refer to hereafter as the potential matrix, see [4], [5] for details. The noncausal field can be represented by an autoregressive (AR) model driven by a correlated noise field, expressed in terms of the potential matrix as

$$A\vec{X} = \vec{v}, \qquad \vec{v} \sim \eta(\vec{0}, \sigma^2 A), \tag{1}$$

where each row of the $N \times M$ lattice is mapped lexicographically into an $M \times 1$ random vector and these are stacked one on top of the other to form the $NM \times 1$ vector, $\vec{X} = [\vec{x}_1^T, \vec{x}_2^T, \cdots, \vec{x}_N^T]^T$, where

CH2977-7/91/0000-2997 $1.00 © 1991 IEEE

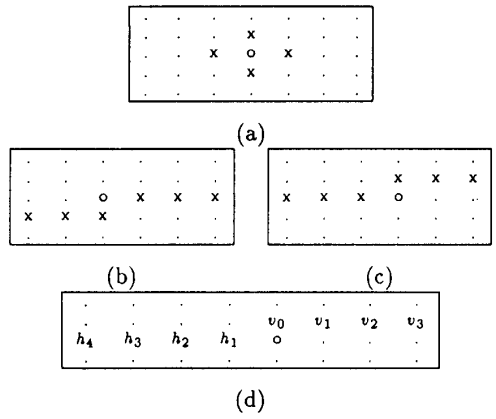

Figure 1: (a) Neighbors for first order noncausal MRF marked by "x". (b) Neighbors for the equivalent backward regressor (c) Neighbors for the equivalent forward regressor (d) Coefficients of the forward regressor.

$\vec{x}_i = [x_{i1}, x_{i2}, \cdots, x_{iM}]^T$. This is equivalent to the minimum variance representation in [6].

Two equivalent one–sided representations can be obtained by a suitable transformation of (1): a "backward" or "anticausal" representation

$$U\vec{X} = \vec{w}, \qquad \vec{w} \sim \eta(\vec{0}, \sigma^2 I). \tag{2}$$

where U is upper triangular, $\vec{w}$ is a white noise vector defined as $\vec{w} = (U^T)^{-1}\vec{v}$, $E(\vec{X}\vec{w}^T) = \sigma^2 U^{-1}$, and a "forward" or "causal" representation which is a mirror image of the "backward" one. Since U is upper triangular, (2) is a "backward" or "anticausal" representation of the field in the sense that any pixel (i,j) depends only on those pixels that lie in its "future". Here "future" and "past" are defined using a Non-Symmetric Half-Plane (NSHP) partitioning at (i,j).

Using the structure of U the representation in equation (2) can be expanded as an $(M \times 1)$ "backward" vector AR process:

$$\begin{aligned} U_i\vec{x}_i + \Theta_i\vec{x}_{i+1} &= \vec{w}_i, \ \ \vec{w}_i \sim \eta(\vec{0}, \sigma^2 I), \ \ i \leq N-1, \\ U_N\vec{x}_N &= \vec{w}_N, \ \ \vec{w}_N \sim \eta(\vec{0}, \sigma^2 I) \end{aligned} \tag{3}$$

where U_i and Θ_i are $M \times M$ blocks, with the U_i's being upper triangular, $\vec{w}_i \perp \vec{w}_j$ for $i \neq j$, $\vec{w}_i \perp \vec{x}_j$ for $i < j$, and $E(\vec{x}_i\vec{w}_i^T) = \sigma^2 U_i^{-1}$ for $1 \leq i \leq N$, i.e., the driving noise $\{w_{i,j}\}$ is white and uncorrelated with all pixels that lie in its "future".

At the pixel level, the result of the above transformation is the replacement of the noncausal neighborhood set by an "anticausal" one. For example, for first order fields, the Θ_i's are lower triangular, so the noncausal neighborhood set of 4 pixels (see Figure 1 (a)) is replaced by an "anticausal" one with M pixels (see Figure 1 (b)). Figure 1 (c) shows the corresponding set for the "forward" or "causal" representation.

The matrices, $\{U_i, \Theta_i\}$, define a set of spatially varying regressors that comprise the equivalent one–sided representation. Defining $\Sigma_i = U_i^T U_i$, the Riccati iterative scheme,

$$\Sigma_i = B - C^T \Sigma_{i-1}^{-1} C, \tag{4}$$

with initial condition $\Sigma_1 = B_1$, is used to compute $\{U_i\}_{i=1}^N$, and the Θ_i's are computed from the corresponding U_i's by using the relationship $U_i^T\Theta_i = C$. The sequence $\{\Sigma_i\}$, defined by (4) converges with a geometric rate of convergence.

As an example, consider a first order noncausal GMRF defined on a 128×128 lattice, assuming free boundary conditions (b.c.), with horizontal interaction parameter $\beta_h = 0.395$, vertical interaction parameter $\beta_v = -0.1$, and field conditional variance $\sigma^2 = 400$. A sample from this field was synthesized using the equivalent "backward" representation (3), which was computed using the Riccati iteration in (4) (see Figure 2 (a)). The geometric rate of convergence of the iteration (4) is of practical importance because it means that convergence of the Riccati equation to any given precision, ϵ, is obtained after a small number of iterations. Using $\epsilon = 10^{-4}$, we obtained convergence at the 10th iteration. The one–sided regressor coefficients were found to decay monotonically with distance from the "present" pixel. The regressor tails are truncated at the pixel at which the coefficient is less than 1% of the first coefficient, i.e, with reference to Figure 1 (d), $h_i \doteq 0$ if $\mid \frac{h_i}{h_1} \mid < 0.01$, and $v_i \doteq 0$ if $\mid \frac{v_i}{v_0} \mid < 0.01$. Consequently, the steady state regressor has 3 neighbors in the same row, with coefficients h_1, h_2, h_3 given by -0.54084, -0.01192, -0.00727, respectively, and 11 in the previous row, with coefficients $v_0, v_1, \ldots, v_{10}$ given by -0.13177, -0.07127, -0.04011, -0.02350, -0.01431, -0.00904, -0.00590, -0.00396, -0.00273, -0.00192, -0.00137, respectively.

3. Recursive enhancement

The noisy image Y is given by

$$y_{i,j} = x_{i,j} + n_{i,j}, \qquad 1 \leq i \leq N, \ 1 \leq j \leq M \tag{5}$$

where $n_{i,j}$ is additive white Gaussian noise independent of the original image pixels $x_{i,j}$. The following procedure is used to compute the optimal MMSE

smoother estimate of the image X, given the noisy image Y.

Step 1. Identification of the noncausal field: The noiseless image is modeled as a noncausal finite lattice GMRF. The parameters of this model are estimated.

Step 2. Equivalent one-sided representation: The set of spatially varying regressors (i.e., $\{U_i, \Theta_i\}$) that comprise the equivalent "backward" or "anticausal" representation (3) are obtained using the Riccati iteration in (4). As demonstrated in the example above, the geometric rate of convergence considerably reduces the computational and storage requirements. The "forward" regressors are easily obtained by reflecting the "backward" regressor matrices.

Step 3. Recursive Smoothing: The equivalent one-sided representation (3) is formulated as a "backward" state space model:

$$\begin{aligned} \vec{x}_i &= F_i^b \vec{x}_{i+1} + G_i^b \vec{w}_i, \qquad 1 \le i \le N-1 \quad (6) \\ \vec{x}_N &= G_N^b \vec{w}_N \end{aligned}$$

where $F_i^b = -U_i^{-1}\Theta_i$ and $G_i^b = U_i^{-1}$. The "forward" state space model is easily obtained from the "backward" one by a series of reflections. This is then used as the basis for the Rauch–Tung–Striebel (RTS) formulation of the optimal fixed interval smoother, see for e.g., [7].

3.1 Experimental Results

The first experiment was conducted using the field that was synthesized in the last section. This field has a predominantly horizontal wood–grain like texture (see Figure 2 (a)). White Gaussian noise of variance 1980 (chosen so that the noisy image had SNR of approximately -3 db) was added to the field producing a noisy image with MSE = 1991 (see Figure 2 (b)). Below, we will use MSE as a form of merit although we have not investigated the issue of field ergodicity and corresponding statistical meaning of this quantity. To provide an upper bound on the enhancement performance the actual field model that was used to synthesize the image was applied as the noncausal model for the enhancement procedure. The equivalent one–sided representation was derived, exactly as described above, and the RTS smoother was applied. The MSE of the enhanced image, shown in Figure 2 (c), was reduced to 461, while retaining the prominent texture characteristics. Although some detail has been lost due to smoothing, the predominant horizontal grain texture of the original field is unobscured by any artifact of the enhancement.

The second experiment was conducted using a 128 × 128 Lenna image (see Figure 3 (a)). White Gaussian noise of variance 630 (chosen so that the noisy image had SNR of approximately 7 db) was added to the field producing a noisy image with MSE = 633 (see Figure 3 (b)). The noiseless image was modeled as a first order GMRF with free b.c., with an ML estimation procedure (to be discussed in a forthcoming paper) being used to estimate the parameters. In practice, the image model parameters have to be estimated from the noisy data, but to simplify the experiment, here we used the original image data. Prior to the processing, the sample mean was subtracted from the image to make it zero mean. The ML parameter estimates obtained were $\widehat{\beta_h} = 0.241857$, $\widehat{\beta_v} = 0.258286$, and $\widehat{\sigma^2} = 137.790778$. Next, the equivalent one–sided representation was computed. Applying the same truncation rule for the regressor coefficients as before, we got a steady state regressor with 6 neighbors in the same row having coefficients $h_1, \ldots h_6$ given by -0.35441, -0.02416, -0.01293, -0.00782, -0.00516, and -0.00363 respectively, and 8 neighbors in the previous row with coefficients $v_0, \ldots, v_7$ given by -0.32191, -0.11409, -0.04821, -0.02400, -0.01366, -0.00860, -0.00582, and -0.00416, respectively (see Figure 1 (d)). The RTS smoother produced an enhanced image with MSE = 168 (see Figure3 (c)).

To contrast the effect of the noncausal image field model with that produced by a causal field, the RTS smoother was applied directly with a 3 neighbor causal model (see Figure 4) whose parameters β_h^c, β_v^c, and β_d^c, representing respectively the West, North, and North–West neighbor interactions, were estimated from the noiseless image using least squares. The estimates obtained were $\widehat{\beta_h^c} = 0.666224$, $\widehat{\beta_v^c} = 0.863320$, $\widehat{\beta_d^c} = -0.556740$, and for the field conditional variance, $\widehat{\sigma_c^2} = 118.731850$. The output of the RTS smoother has MSE = 155 (see Figure 3 (d)) which is slightly better than the MSE of the enhanced field produced using a noncausal model, but a visual comparison (see Figure 3 (c) and (d)) reveals that the causal model produced streaking in the enhanced image while the noncausal model did not. This underlies the importance of utilizing a noncausal image model.

4. Conclusions

The main point of the paper is that is possible to apply recursive optimal procedures for image processing without sacrificing the important field model property of noncausality. Currently, work is in progress to enable the identification of the noiseless image model parameters from the noisy data. Another issue that is under investigation is the segmentation of the image into homogeneous regions, each of which can be modeled as a homogeneous GMRF and processed accordingly.

References

[1] J. E. Besag. Spatial interaction and the statistical analysis of lattice systems (with discussion). *J. R. Stat. Soc., B*, 36(2):192–236, 1974.

[2] S. Geman and D. Geman. Stochastic relaxation, Gibbs distribution, and Bayesian restoration of images. *IEEE Trans. Pattern Anal. Machine Intell.*, PAMI-6:721–741, November 1984.

[3] J.W. Woods and C.H. Radewan. Kalman filtering in two dimensions. *IEEE Trans. Inform. Theory*, IT-23(4):473–481, July 1977.

[4] José M. F. Moura and Nikhil Balram. A recursive framework for noncausal Gauss Markov random fields. In *24th Annual Conf. Inform. Sci. Syst.*, Princeton, NY, March 1990.

[5] José M. F. Moura and Nikhil Balram. Recursive structure of noncausal Gauss Markov random fields. Technical Report 90-08, LASIP, ECE,Carnegie Mellon University, 43 pages, June 1990. Submitted for publication.

[6] J.W. Woods. Two-dimensional discrete Markovian fields. *IEEE Trans. Inform. Theory*, IT-18:232–240, 1972.

[7] A. Gelb, editor. *Applied Optimal Estimation*. The M.I.T. Press, Cambridge, Massachusetts, 1974.

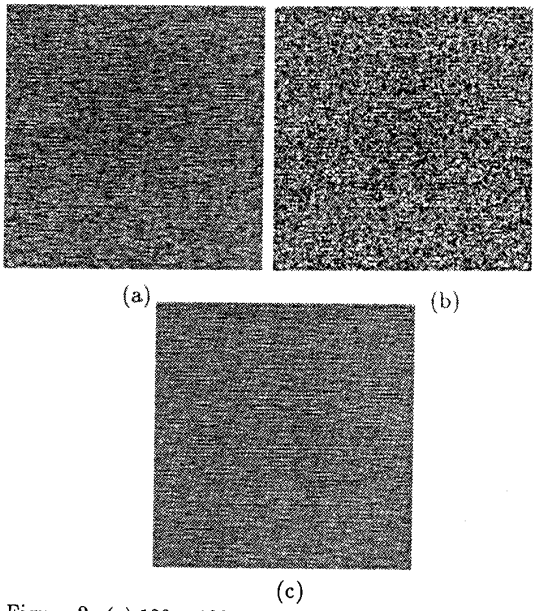

Figure 2: (a) 128 × 128 sample of 1st order GMRF with $\beta_h = 0.395$, $\beta_v = -0.1$, $\sigma^2 = 400$ (b) Synthesized image with -3 db noise added: MSE = 1991 (c) Image enhanced using noncausal field model: MSE = 461.

x x
x o

Figure 4:Neighbors for causal field model marked by"x".

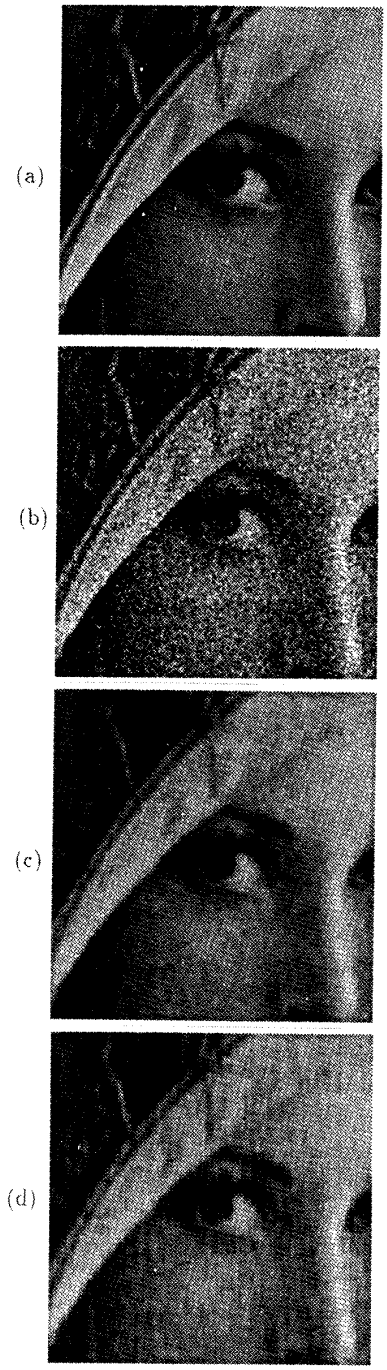

Figure 3: (a) 128 × 128 Lenna (b) Lenna with 7db noise added: MSE = 633 (c) Image enhanced using noncausal field model: MSE = 168. (d) Image enhanced using causal field model: MSE = 155.